

Molecular Dynamics Simulation of the Melting Process in Au₁₅Ag₄₀ Nanoalloys

F. Arianfar, R. Rostamian and H. Behnejad*

Department of Physical Chemistry, School of Chemistry, University College of Science, University of Tehran, Tehran, Iran

(Received 14 December 2016, Accepted 17 January 2017)

In this study, the operations of melting Au₁₅Ag₄₀ nanoalloy is studied using the molecular dynamics simulation through the Gupta multiparticle potential and the nonergodicity of simulation is eliminated by the multiple histogram method. The melting characteristics were specified by the analysis of differences in the potential energy. The calculations indicated that the melting of Au₁₅Ag₄₀ nanoalloy starts at 470 K and then rises to peak at 505 K and at about 600 K the total Au₁₅Ag₄₀ is melted. We also obtained the Lindemann parameter and other properties at several temperatures during the simulation. The power spectrum values at zero frequency were used to show the intensity of diffusive motions at the given temperature.

Keywords: Nanoalloys, Molecular dynamics simulation, Melting mechanism, Gupta many body model, Multiple histogram method

INTRODUCTION

Nanostructure materials are a part of big scientific topic because they present specific and unique properties. Indeed, at nanoscale ranges the unique properties which are size-dependent are usually observed. Generally, bimetallic nanoalloys are known as very interesting materials in nanoscale because their characteristics can be easily altered by varying their size. Moreover, their composition can be adjusted to obtain some new properties [1-3]. They have many methodology for microscopic modeling on the molecular level. Moreover, the nature of matter is put in the solution of the *N*-body problem [4-7].

Bimetallic nanoparticles or nanoalloys are clusters of metallic atoms that have attracted great attention because of their application in various research areas, including optics, catalysis, bio-diagnostics and magnetism. According to the literature, one of the most important attributes of nanoscale systems is the thermal stability, so, studying the melting mechanism of nanoalloys has received high attention from the experimental and computational point of view as well [2].

To study the thermal and structural properties of the nanoalloys, some investigations have been carried out, though they are often about finding the most stable configuration namely the global minimum using the different methods (such as genetic algorithm) [8]. The global minimum structure of nanoalloy shows the starting structure to understand the behavior of melting which is one of the main topics about nanoalloys [9-11].

According to the literatures, there is a little study about melting mechanism of nanoalloys. Alavi has reported MD simulation to characterize the melting points of Al nanoparticles (55-1000 atoms) with the Streitz-Mintmire variable-charge electrostatic plus potential. They found out that nanoparticles containing \leq under 850 atoms show bi-stability between the liquid and solid phases in temperature ranges under the point of complete melting [2]. In 2011, Shi *et al.* published a MD simulation study to simulate the freezing and melting of Au-Pt nanoalloy confined in single-walled carbon tubes (SWNTs). Their simulation results demonstrate that the clusters have multi-shell structures in both melted and confined clusters and Pt atoms tend to stay at the position close to the SWNT wall.

Our previous study has published MD simulation for understanding the melting mechanism of Ag₂₇Cu₁₃

*Corresponding author. E-mail: h.behnejad@ut.ac.ir

nanoalloy using thermodynamical, geometrical and dynamical criteria in NVT ensemble coupled to steepest descent quenching method [11].

In the current study, the melting mechanism of Au₁₅Ag₄₀ nanoalloy is defined by MD simulation.

METHODOLOGY

Potential Model

In this work, we have used the second moment approximation (abbreviated as SMA) tight-binding analytic potential [12], which is mostly employed in thermal and structural studies of metal clusters. In this model, the whole energy is obtained by:

$$E = \sum_j E_j^b + E_j^r, \quad (1)$$

where, E_j^b is the bonding and E_j^r is the repulsive Born-Mayer term. These two terms for binary system consisting α and β type atoms are expressed as:

$$E_j^b = -\sqrt{\sum_i \zeta_{\alpha\beta}^2 \exp\left[-2q_{\alpha\beta}\left(\frac{r_{ij}}{r_0} - 1\right)\right]}, \quad (2)$$

$$E_j^r = \sum_i A_{\alpha\beta} \exp\left[-p_{\alpha\beta}\left(\frac{r_{ij}}{r_0} - 1\right)\right], \quad (3)$$

Where α and β represent the atomic species i and j , respectively, and r_0 is the nearest-neighbor equilibrium distance in the pure metals (Au and Ag). The parameters (A , ζ , p , q) for homometallic interaction (Ag-Ag and Au-Au) is given by fitting to the experimental data values. The Potential parameters for the interaction between two different atoms are defined as the geometric average of the two distinct atoms for A and ζ and arithmetic averages for p , q and r_0 . The Gupta parameters for simulation of Ag-Au nanoalloys are tabulated in Table 1 [8].

Simulation Method

Global minimum structures of Au₁₅Ag₄₀ taken from the work of Xiangjing *et al.* [13-15], were used as an initial configuration to perform simulations at various

temperatures using DL-POLY simulation package [16]. Potential parameters were determined by Gupta [17,18,8], and then applied to simulate the interaction between the atoms. In our simulation study the constant temperature ensemble (NVT), the velocity version of the Verlet algorithm [10] and Evans thermostat [7] were employed. Time step of simulation was 1 fs and instant positions as well as velocities of the atoms were recorded every 10 fs. The cutoff distance was 14 Å. Instant atom positions and velocities were placed on file every 10 femtosecond. MD simulations were performed from 50 to 700 K in an increment of 20 K but the increment was reduced to 10 K near the coexistence range. Nevertheless, as it will be described later, extending the simulation time duration cannot further improve the statistical precision of the results and the heat capacity up to this time present strong fluctuations in the coexistence phase region. Hence, we applied the weighted histogram analysis method to succeed in non-ergodicity in the phase coexistence region.

Different methods used to find out the melting mechanism of the nanoalloys classified into three groups: thermodynamical (caloric curve and heat capacity), geometrical (the distance fluctuation criterion, radial distribution function) and dynamical (velocity autocorrelation function and power spectrum) quantities.

Caloric curve was utilized as a thermodynamical criterion to indicate the melting transition to have a generalized illustration of the melting process. To determine the melting point, the usage of heat capacity values versus temperature is preferred because they are more precise to exhibit such behaviors. To examine environment similarity of the atoms as the temperature increases, velocity autocorrelation function and its Fourier transform and power spectrum are used. Moreover, diffusive motions can be ascertained by nonzero values of the power spectrum at zero frequency ($\omega = 0$).

Thermodynamics Criteria

Heat capacity and caloric curve. Caloric curve and heat capacity are two familiar criteria usually utilized to identify the melting transition. Caloric curve is the time average of the potential energy values throughout the simulation against temperature. For the solid or liquid phases, the caloric curve is a gradual increasing function

Table 1. The Gupta Potential Parameters

	A	r_0 (\AA)	ζ (eV)	p	q
Au-Au	0.2096	2.8850	1.8153	10.139	4.033
Ag-Au	0.1488	2.8885	1.4874	10.494	3.607
Ag-Ag	0.1031	2.8921	1.1895	10.850	3.180

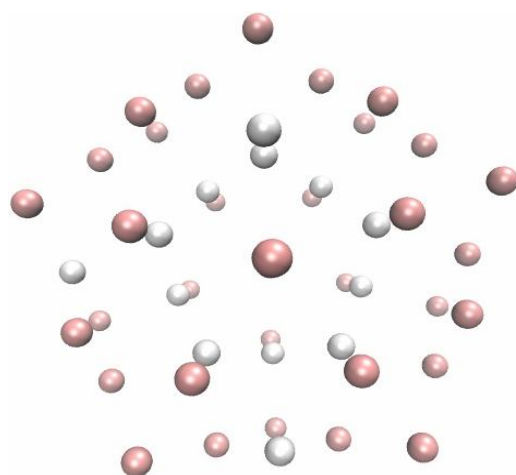


Fig. 1. The geometry of the global minimum of $\text{Au}_{15}\text{Ag}_{40}$ nanoalloy. Ochre and silver balls represent Ag and Au atoms, respectively.

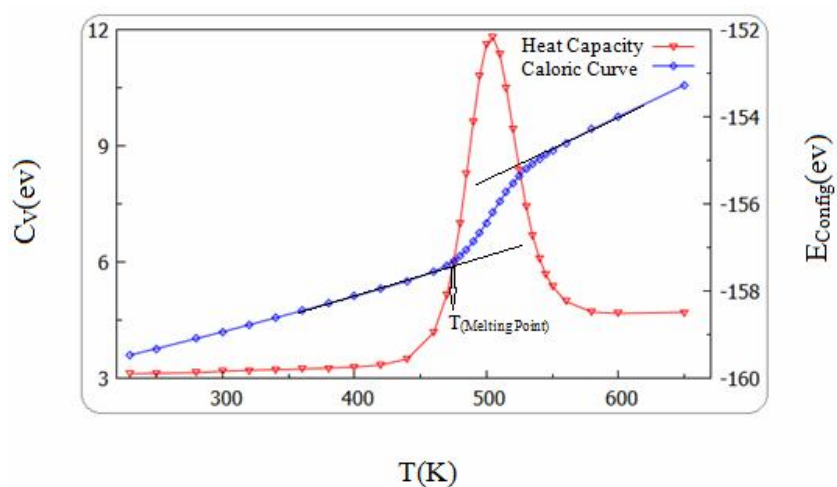


Fig. 2. Heat capacity and Caloric Curve of $\text{Au}_{15}\text{Ag}_{40}$ nanoalloy as a function of temperature.

of temperature. As for coexistence region, the caloric curve generally displays a drastically alteration related to the latent heat.

The constant volume heat capacity, C_v , is another thermodynamical criterion to study the melting process in nanoalloy. While bulk solid materials normally show singularity in the C_v vs. temperature within phase transition, nanoparticles show one or more softened peaks at a range of temperature.

The heat capacity in the canonical ensemble is defined as the fluctuation of the energy [4,19]:

$$C_v(T) = \frac{3}{2}Nk_B + \frac{\langle E^2 \rangle - \langle E \rangle^2}{k_B T^2}, \quad (4)$$

where E is the potential energy, k_B is the Boltzmann constant and N is the number of atoms.

Concerning to quasi-ergodicity subject matters, the equilibrium properties (like the heat capacity) do not converge and keep fluctuate as a function of simulation time. To come down in support of these fluctuations, we used a histogram analysis [20-23]. Hence, this method can be used to obtain equilibrium properties of a system at non-ergodic conditions by averaging over the results of the ergodic conditions [24-26].

RESULTS AND DISCUSSION

Figure 1 shows the geometry (C_1 symmetry) and structure of the global minimum of $Au_{15}Ag_{40}$ corresponding to a core shell nanoalloy because of the bigger radius and lower surface energy of the Ag atoms with respect to the core Au atoms [14].

A Gupta like potential was applied to the tight binding model to mimic the interactions between the atoms of the nanoalloy based on the second moment approximation [12]. This shows a seamless study of static structures by the Birmingham cluster genetic algorithm (BCGA) program and dynamical behavior on long time scales [20,23,26,11]. After performing the MD simulation at different temperatures, we should have a decisive factor to determine melting mechanism.

Figure 2 shows the value of C_v change vs. temperature. The equilibrium properties (such as the heat capacity) do

not converge and keep fluctuating as a function of simulation time (in non-ergodicity topic). To eliminate these fluctuations, particularly in the C_v case near the melting region we used a histogram analysis method [20,23,26,11].

Also, in this figure two changes are in its slope at approximately 470 K and 550 K. The relationship between these temperatures and the melting points of shell and core atoms of the nanoalloy should be understood. Although, the caloric values are in a good agreement with both high and low temperatures. They have strong fluctuations at intermediate temperature range. For the further understand the melting mechanism in detail other criteria was studied as follow.

Figure 3 presents the values of δ versus temperature for the whole atoms of the $Au_{15}Ag_{40}$ nanoalloy. At temperature around 505 K, a sudden increase in δ values occurs and this behavior continues until around 600 K. From this temperature upward, the rate of change in δ decreases and finally at around 650 K settles down and becomes constant. So, we can infer that the melting happens at this point. Since below the melting point temperatures atoms oscillate around their equilibrium positions, thus in the solid region the values of δ generally undergo gradual and, nearly, linear changes as the temperature increases then ascend precipitously in the transition region as the clusters begin to gain enough energy to surmount the potential barriers to rearrange and then calm down partly in the liquid region. As we previously reported, the range of melting depends on the size of the system [11].

Figure 4 shows the RDF of $Au_{15}Ag_{40}$ nanoalloy for different pairs of atoms (Au-Au, Au-Ag and Ag-Ag) at various temperatures. RDF can be explained as the probability of finding an atom at a distance (r) from other atom in comparison to a homogeneous distribution. It displays that Ag is not overall miscible with Au. If they were miscible and form a homogeneous mixture, the radial distributions of Au-Au would widen to the cluster diameter. At low temperature, the curves characterize the solid structure while at higher temperature they present the liquid behavior.

Figures 5 and 6 show the dynamical behavior of $Au_{15}Ag_{40}$ as the temperature increases using VACF and power spectrum of the constituent atoms of $Au_{15}Ag_{40}$, respectively. For $Au_{15}Ag_{40}$, the similarity of the behavior

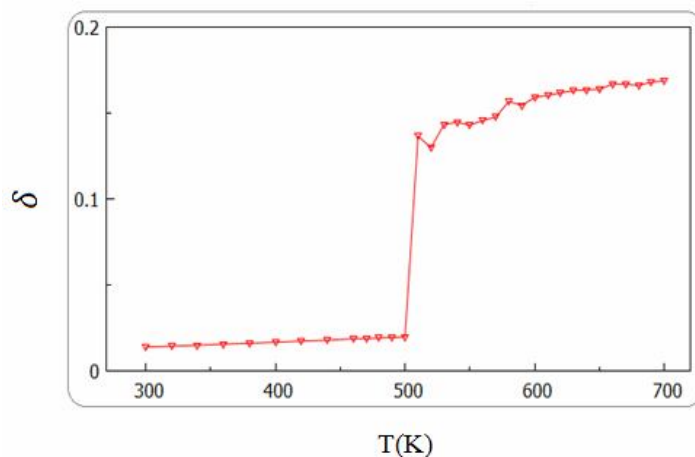


Fig. 3. The root mean square bond length fluctuation as a function of temperature.

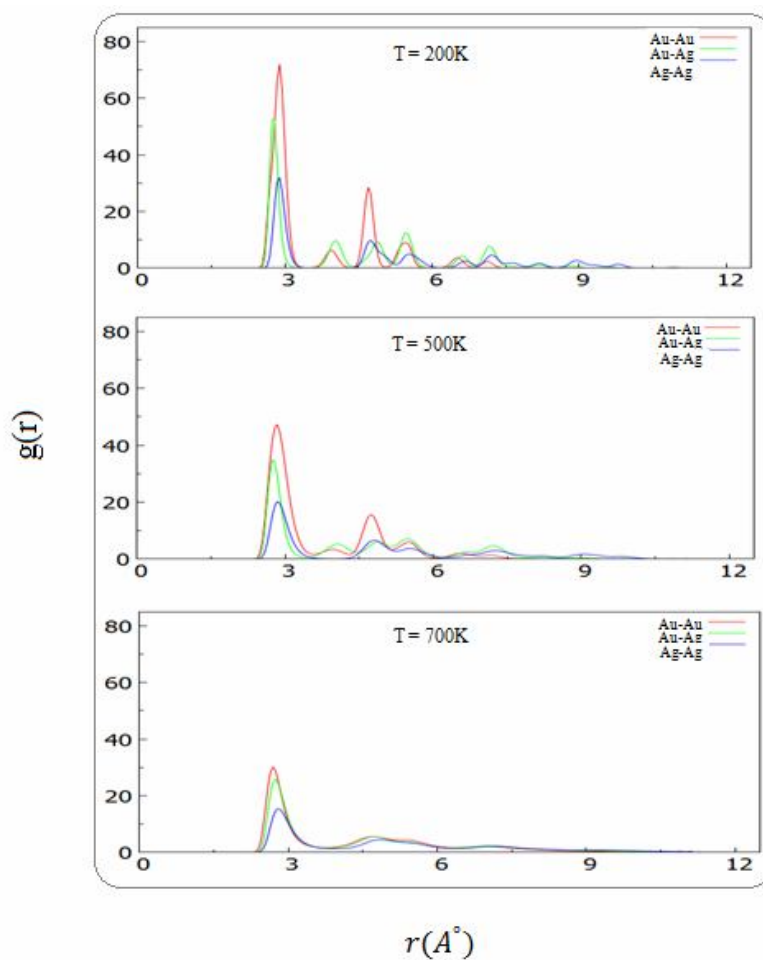


Fig. 4. Radial distribution functions for different pairs of atoms of $\text{Au}_{15}\text{Ag}_{40}$ nanoalloy at different temperatures.

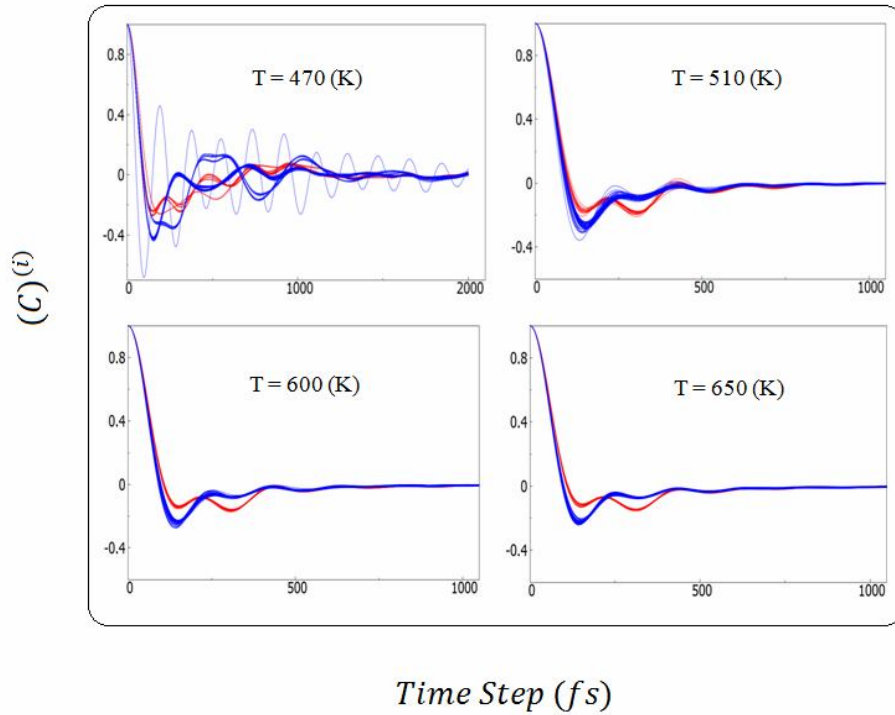


Fig. 5. Velocity auto correlation functions vs. time for all constituents of the Au₁₅Ag₄₀ nanoalloy at different temperatures. (Red lines are for Au and blue lines are for Ag atoms).

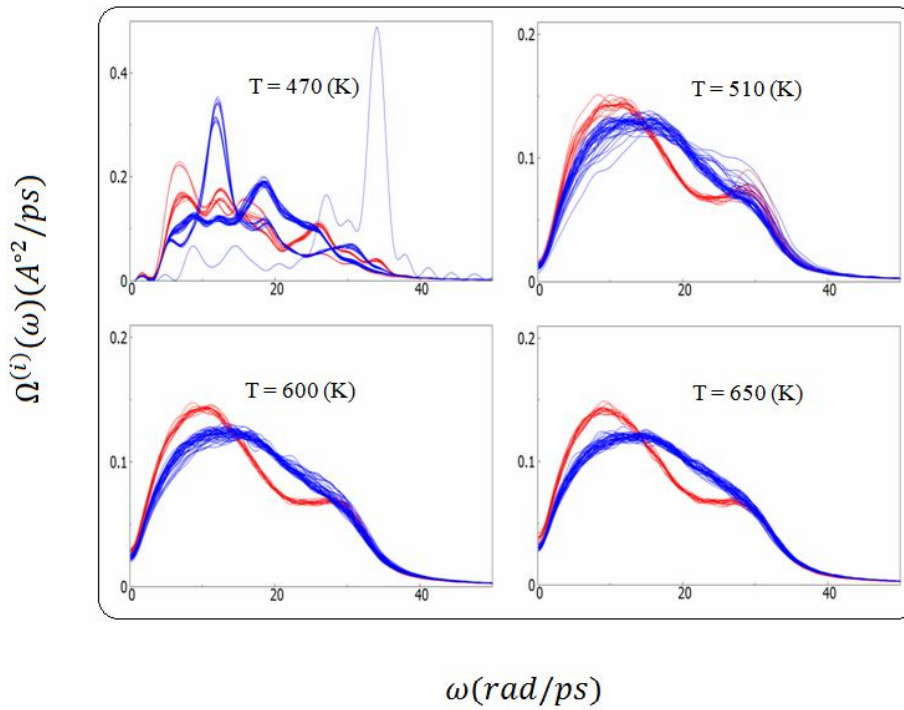


Fig. 6. Power spectra vs. frequency at different temperatures which red lines are for Au and blue lines are for Ag atoms.

increases as the temperature goes up until at melting temperature where the curves for the shell atoms and core atoms merge into two single curves. Power spectrum is, also, as an indicator for the beginning of diffusive motions with taking nonzero values at zero frequency and increasing its value as the melting behavior intensifies. As seen, as the temperature goes up, the value of the power spectrum at zero frequency increases, indicating diffusive motions occurring in the system. It is useful to point out that at low temperature the more oscillating atom in the VACF curve has the highest frequency.

CONCLUSIONS

In this study, several complementary procedures were used to research the melting mechanisms of Au₁₅Ag₄₀ nanoalloy by the MD simulation method at constant temperature. The global minimum energy structure of Au₁₅Ag₄₀ was initially used to study its melting behavior exploiting by means of thermodynamical, dynamical and geometrical criteria. Caloric curve and heat capacity were utilized as thermodynamical factor to present the melting transition. In the phase coexistence region, fluctuations are observed through these quantities. It is the evidences for the non-ergodic behavior of the system at above temperatures. Therefore, the multiple histogram technique were utilized to overcome the non-ergodicity issue [20,23,26,11].

When the Au₁₅Ag₄₀ nanoalloy temperature is raised in order to study its melting behavior, two types of processes might be created; solid-solid and solid-liquid transitions. Values of the Lindemann parameter at various temperatures give increasing at a slow speed and nearly continuous variations in a wide temperature range for all nanoalloys where the total melting occurs, in accordance with results obtained from heat capacity curve. The VACF and power spectrum curves show that the similarity in the behavior of the atoms increases as the temperature increases. Atoms subjected to stronger forces exhibit more oscillating behavior in their VACF curves and correspondingly higher frequency in the power spectrum curve. Moreover, the power spectrum values at zero frequency can be utilized to show the intensity of diffusive motions at the given temperature.

ACKNOWLEDGEMENTS

Authors are very indebted to research committee of the University of Tehran due to its authorities for financial support until research was done.

REFERENCES

- [1] Hsu, P.; Luo, J.; Lai, S.; Wax, J.; Bretonnet, J. -L., Melting scenario in metallic clusters. *J. Chem. Phys.* **2008**, *129*, 194302, DOI: 10.1063/1.3009194.
- [2] Alavi, S., Molecular dynamics simulations of the melting of aluminum nanoparticles, *J. Phys. Chem. A*, **2006**, *110*, 1518-1523, DOI: 10.1021/jp053318s.
- [3] Shi, R.; Shao, J.; Zhu, X.; Lu, X., On the melting and freezing of Au-Pt nanoparticles confined in single-walled carbon nanotubes. *J. Phys. Chem. C*, **2011**, *115*, 2961-2968, DOI: 10.1021/jp109689m.
- [4] Ferrando, R.; Jellinek, J.; Johnston, R. L., Nanoalloys: from theory to applications of alloy clusters and nanoparticles. *Chem. Rev.* **2008**, *108*, 845-910, DOI: 10.1021/cr040090g.
- [5] Haile, J. M., Molecular dynamics simulation: elementary methods. John Wiley & Sons, Inc.: 1992.
- [6] Rapaport, D. C., The art of molecular dynamics simulation. Cambridge university press: 2004.
- [7] Keshavarz, F.; Mohammad-Aghaie, D., Dual-target anticancer drug candidates: Rational design and simulation studies. *Phys. Chem. Res.* **2015**, *3*, 125-143, DOI: 10.22036/pcr.2015.8158.
- [8] Gupta, R. P., Lattice relaxation at a metal surface. *Phys. Rev. B* **1981**, *23*, 6265-6270, DOI: 10.1103/PhysRevB.23.6265.
- [9] Li, Y.; Blaisten-Barojas, E.; Papaconstantopoulos, D., Structure and dynamics of alkali-metal clusters and fission of highly charged clusters. *Phys. Rev. B* **1998**, *57*, 15519-15532, DOI: 10.1103/PhysRevB.57.15519.
- [10] Verlet, L., Computer "experiments" on classical fluids. I. Thermodynamical properties of Lennard-Jones molecules. *Phys. Rev.* **1967**, *159*, 98-103, DOI: 10.1103/PhysRev.159.98.
- [11] Asgari, M.; Behnejad, H., Molecular dynamics simulation of the melting process in Ag₂₇Cu₁₃ core-shell nanoalloy. *Chem. Phys.* **2013**, *423*, 36-42, DOI:

- 10.1016/j.chemphys.2013.06.014.
- [12] Cleri, F.; Rosato, V., Tight-binding potentials for transition metals and alloys. *Phys. Rev. B*, **1993**, *48*, 22-33, DOI: 10.1103/PhysRevB.48.22
- [13] Wales, D.; Doye, J.; Dullweber, A.; Hodges, M.; Naumkin, F.; Calvo, F.; Hernández-Rojas, J.; Middleton, T., The cambridge cluster database. URL <http://www-wales.ch.cam.ac.uk/CCD.html>, 2001, 117.
- [14] Lai, X.; Xu, R.; Huang, W., Geometry optimization of bimetallic clusters using an efficient heuristic method. *J. Chem. Phys.* **2011**, *135*, 164109, DOI: 10.1063/1.3656766.
- [15] Mohn, C. E.; Stølen, S.; Kob, W., Predicting the structure of alloys using genetic algorithms. *Mater. Manuf. Process.* **2011**, *26*, 348-353, DOI: 10.1080/10426914.2011.552021.
- [16] Smith, W.; Forester, T., The DL_POLY package of molecular simulation routines. Daresbury UK: Daresbury and Rutherford Appleton Laboratory: 1996.
- [17] Chen, F.; Curley, B. C.; Rossi, G.; Johnston, R. L., Structure, melting, and thermal stability of 55 atom Ag-Au nanoalloys. *J. Phys. Chem. C* **2007**, *111*, 9157-9165, DOI: 10.1021/jp0717746.
- [18] Chen, F.; Johnston, R. L., Energetic, electronic, and thermal effects on structural properties of Ag-Au nanoalloys. *ACS nano*. **2007**, *2*, 165-175. DOI: 10.1021/nm700226y.
- [19] Proykova, A.; Berry, R., Insights into phase transitions from phase changes of clusters. *J. Phys. B* **2006**, *39*, R167, DOI: 10.1088/0953-4075/39/9/R01.
- [20] Ferrenberg, A. M.; Swendsen, R. H., Optimized monte carlo data analysis. *Phys. Rev. Lett.* **1989**, *63*, 1195-1198, DOI: 10.1103/PhysRevLett.63.1195.
- [21] Asgari, M.; Behnejad, H., Molecular dynamics simulation of the melting process in Ag₂₇Cu₁₃ core-shell nanoalloy. *Chem. Phys.* **2013**, *423*, 36-42, DOI: 10.1016/j.chemphys.2013.06.014.
- [22] Oderji, H. Y.; Ding, H., Determination of melting mechanism of Pd₂₄Pt₁₄ nanoalloy by multiple histogram method *via* molecular dynamics simulations. *Chem. Phys.* **2011**, *388*, 23-30, DOI: 10.1016/j.jcp.2009.05.011.
- [23] Bereau, T.; Swendsen, R. H., Optimized convergence for multiple histogram analysis. *J. Comput. Phys.* **2009**, *228*, 6119-6129, DOI: 10.1016/j.jcp.2009.05.011.
- [24] McQuarrie, D.: Statistical mechanics, Happer and Row, New York: 1976.
- [25] Lindemann, F. A., The calculation of molecular vibration frequencies. *Phys. Z.* **1910**, *11*, 609-612.
- [26] Oderji, H. Y.; Ding, H., Determination of melting mechanism of Pd₂₄Pt₁₄ nanoalloy by multiple histogram method *via* molecular dynamics simulations. *Chem. Phys.* **2011**, *388*, 23-30, DOI: 10.1016/j.chemphys.2011.07.011.